

Laser ignition of high-energy materials containing AlB_2 and AlB_{12} powders

Alexander Korotkikh^{1,2,*}, Konstantin Slyusarskiy¹, Konstantin Monogarov¹, and Ekaterina Selikhova¹

¹National Research Tomsk Polytechnic University, 634050 Tomsk, Russia

²Tomsk State University, 634050 Tomsk, Russia

Abstract. Boron-containing substances are known to have high gravimetric and volumetric heats of oxidation in comparison with any metals that make them promising for using in high-energy materials. This work is aimed to study ignition characteristics of ammonium perchlorate and nitrate-based composite solid propellants containing aluminium borides by means of radiative heating by CO_2 -laser. It was found that the effect upon laser ignition (ignitability) at full replacement of ASD-4 aluminum powder by aluminium diboride and dodecaboride is close. The ignition time of HEM is reduced by 2.0–2.5 times compared with ASD-4 HEM sample in the heat flux density range of 90–200 W/cm^2 .

1 Introduction

Boron and its compounds are considered to be fuel components with high efficiency for use in solid propellants for solid fuel rocket and ramjet engines [1–3]. Boron hydrides and organic derivatives have the high burning rates in a wide range of oxidizing medium compositions and pressure values. The specific heat of complete boron oxidation in the pure oxygen is more than 1.9 times higher compared to aviation kerosene and aluminum.

The most widespread solid propellant contents 22 wt. % of micro-sized aluminium powder. According to [4, 5] the composite fuel combustion is strongly influenced by presence of aluminium oxide and carbonaceous residues in refractory layer of aluminium powder during oxidation. Aluminium oxide melting point is significantly higher compared to pure aluminium. According to the study [4, 5] the aluminum oxidation during the combustion of composite solid propellants strongly influence by the presence on the burning surface the refractory layer containing the aluminum oxide particles and carbonaceous residues. Melting point of alumina significantly above the melting point of aluminum. The aluminum particles combustion possible at the high temperature gradient of high-energy materials (HEMs) reaction layer near the burning surface with occurrence of cracks and destruction of the oxide layer resulting in the oxidation of active metal. It is well known [6] that the destruction of the aluminum oxide layer on the particle surface may react with the carbon particles to form aluminum carbide.

* Corresponding author: korotkikh@tpu.ru

However, HEMs, containing aluminum micropowders, have the long ignition time and the low burning rate compared to HEMs, containing ultrafine powders of aluminum and other metals [7–10].

This paper presents the experimental dependences of the ignition time and temperatures on heat flux density, the activation energy values for the model HEMs based on ammonium perchlorate and nitrate, energetic binder, containing micron powders of aluminum, aluminium diboride and aluminium dodecaboride.

2 Experimental

2.1 HEM samples

Three HEM samples were used in current study. The first sample (marked as ASD-4) contain ammonium perchlorate (fraction with particle size 160-315 μm), ammonium nitrate (fraction $<50 \mu\text{m}$), energetic binder MPVT-ASP and 30 wt. % of aluminum micron powder ASD-4. Two other samples ASD-4 aluminum was completely substituted by aluminum diboride and aluminium dodecaboride micron powders for samples AIB₂ and AIB₁₂, respectively.

2.2 Ignition of HEM

The ignition process was studied via setup for the radiant heating based on CO₂-laser with the 10.6 μm wavelength and 200 W power (Fig. 1). Before measurements all samples were cut into tablets of 5 mm in height.

The test HEM sample (6) was attached to the sample holder (8). After opening of the shutter (4) radiation was focused by the sodium chloride lens (4) on the HEM sample (6). Signals from photodiodes (7) were transmitted to the L-card-E 14-440 ADC (9) and recorded in the personal computer (10), and then processed with the software application LGraph2. The ignition time t_{ign} of HEMs was determined by difference between the moments of signals from two photodiodes (7), one of which registered the appearance of flame near the end surface of HEM sample. The ignition delay time of HEM samples were determined in atmospheric conditions. Thermo imaging was realized via thermal imager Jade J530 SB.

Video and thermal-imaging was manually started before opening the shutter and stopped after closing the shutter. Files of video and thermal imaging were synchronized with photodiode data by characteristic sound. The relative error of delay times measuring of t_{ign} was equal 5–12 % at the value of confidence probability 0.9.

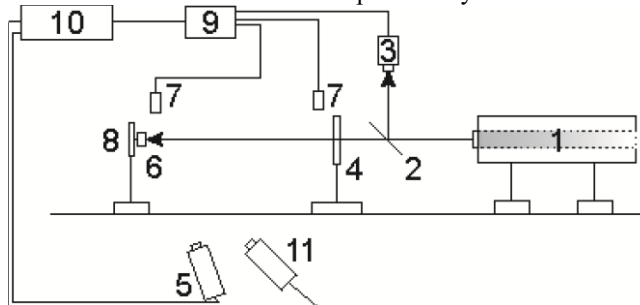


Fig. 1. The scheme of experimental setup based on CO₂-laser: 1 – CO₂-laser; 2 – beam-splitting mirror; 3 – thermoelectric sensor of radiation power; 4 – shutter; 5 – videoimaging camera; 6 – HEM sample; 7 – photodiodes; 8 – sample holder; 9 – ADCs; 10 – PC; 11 – thermal imager.

The radiation power and heat flux density of CO₂-laser beam was measured by the thermoelectric sensor of radiation power (3). The maximum radiation power was defined in the center of the laser beam using a diaphragm with diameter 2 mm. The diameter of the laser beam incident on a HEM sample was 10 mm.

3 Results and discussion

The dependences of HEM ignition time vs. the heat flux density value (in the centre of the laser beam) were determined (Fig. 2).

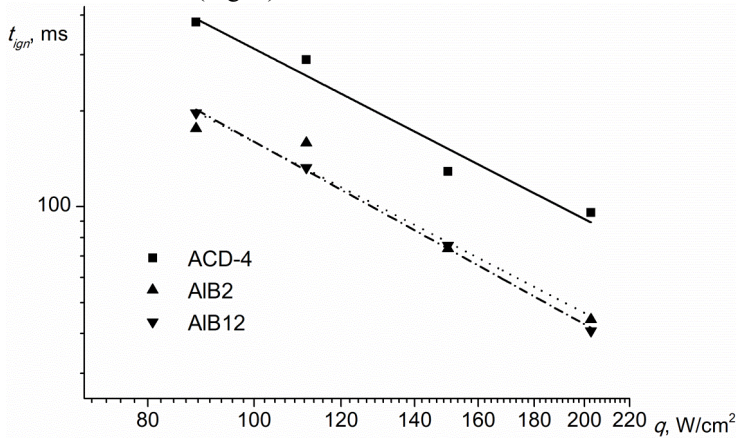


Fig. 2. The ignition time vs. the heat flux density for HEM samples.

It was found that a complete replacement of aluminium by aluminium boride powder in HEM leads to a decrease the ignition time by 2–2.5 times in the heat flux density range of 90–200 W/cm². It is worth mentioning that no significant difference were observed for AIB₂ and AIB₁₂ samples.

Surface average and maximal temperature dependences on time for all samples are given in fig. 3.

Based on presented in Fig. 3 curve slope it could be concluded that AIB₁₂ and AIB₂ samples have close values of heat capacity, while for ASD-4 sample it is greater. It is worth mentioning that gaseous gasification products has strong influence on measured surface temperature value.

The kinetic constants of HEM ignition were determined using following equation [11]:

$$t_{ign} = 0.359 \left(1 - \frac{T_0}{T_{ign}} \right)^2 \frac{E_a c_p}{RQz} \exp \left(\frac{E_a}{RT_{ign}} \right),$$

where E_a is the activation energy, R is the universal gas constant, Q is the specific (per unit weight) heat of reaction, z is a pre-exponential factor, T_{ign} is the quasi-steady ignition temperature that is determined from the condition of equality between the rate of heat supply from reaction layer of chemical interactions and the rate of heat removal into the depth of condensed phase

$$T_{ign} = T_0 + 1.2q \sqrt{\frac{t_{ign}}{\lambda c_p \rho}},$$

where λ , c_p , ρ are factors of the thermal conductivity, the specific heat capacity, and the density for condensed HEM.

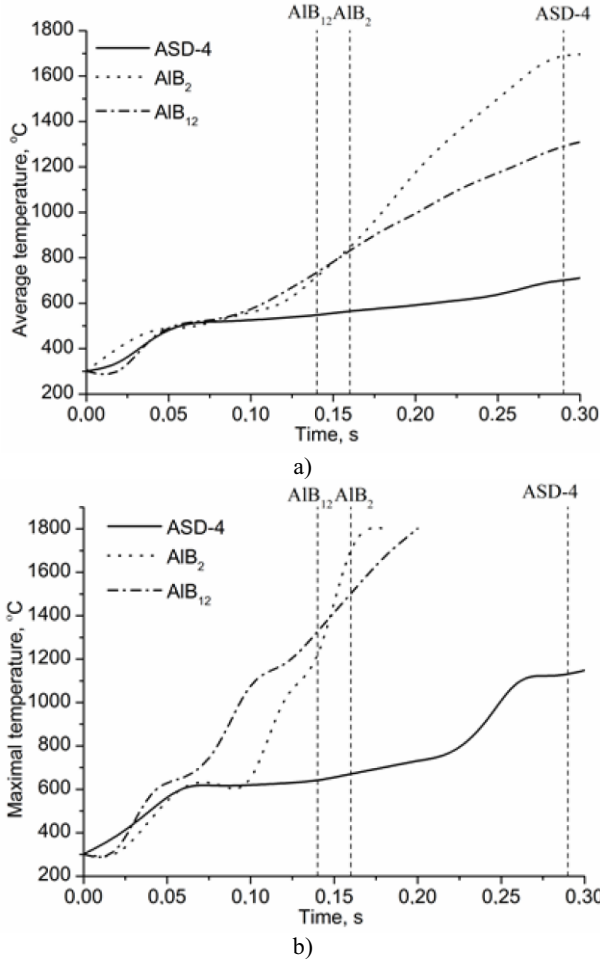


Fig. 3. Dependence of average (a) and maximal (b) surface temperature for HEM samples on time.

The results of calculation of the kinetic constants of ignition for tested HEM samples are presented in Table 1. Here there are values of the average \bar{T} and maximum T_{max} surface temperature on the HEM reaction layer at the ignition moment and appearance of visible flame obtained using a thermal imager Jade J530 SB at $q = 114 \text{ W/cm}^2$. The characteristic parameters of ignition process from Table 1 reveals that there are little difference between average surface temperatures in the moment of ignition while maximal temperatures differ significantly. Despite lower ignition delay times for samples with aluminium dodecaboride the activation energy for this sample was calculated to be lower than for ASD-4 sample due to high Q_z value. Opposite could be said for AIB₂ sample.

Table 1. The activation energy, specific heat of reaction, ignition temperature and surface temperature of the reaction layer for HEM samples.

Parameter	HEM sample, containing metal powder		
	ASD-4	AIB ₂	AIB ₁₂
E_a , kJ/mol	219	98	307
Q_z , W/g	$8.768 \cdot 10^{10}$	$5.136 \cdot 10^6$	$4.811 \cdot 10^{18}$

T^* , K	1684	1114	1744
\bar{T} , K	983±75	990±75	1008±75
T_{\max} , K	1421±120	1973±120	1600±120

4 Conclusions

The ignition parameters for the model HEM samples based on ammonium perchlorate and nitrate, energetic binder, containing micron powder of aluminium, aluminium diboride and aluminium dodecaboride are presented. It was found that the effect upon laser ignition (ignitability) at full replacement of ASD-4 by both aluminium diboride and dodecaboride is close. The ignition time of HEM is reduced by 2.0–2.5 times in the heat flux density range of 90–200 W/cm².

Characteristic temperatures were obtained as well. Average surface temperature at the moment of ignition was found to be nearly same for all studied HEM samples (close to 1000 K) while maximal temperatures differ significantly – they were found to be in range of 1400–2000 K. When replacing the ASD-4 aluminum powder by aluminum dodecaboride in HEM composition the activation energy is increased by 1.4 times and is decreased by 2.25 times for aluminium diboride HEM.

The reported study was partially supported by Russian Scientific Foundation, Grant 16-19-10316.

References

1. A. Gany, Y.M. Timnat, *Acta Astronautica*, **29**, 3 (1993)
2. T.L. Connell, G.A. Risha, R.A. Yetter, C.W. Roberts, G. Young, *Journal of Propulsion and Power*, **31**, 1 (2015)
3. K.-L. Chintersingh, M. Schoenitz, E.L. Dreizin, *Combustion and Flame*, **173** (2016)
4. P.F. Pokhil, A.F. Belyaev, Yu.V. Frolov, V.S. Logachev, A.I. Korotkov, *Combustion of Powdered Metals in Active Media* (Science, Moscow, 1972) [in Russian]
5. V.E. Zarko, O.G. Glotov, *Science and Technology of Energetic Materials*, **74** (2013)
6. A.A. Gromov, A.G. Korotkikh, A.P. Il'in, L.T. DeLuca, V.A. Arkhipov, K.A. Monogarov, U. Teipel, *Nanometals: Synthesis and Application in Energetic Systems, Energetic Nanomaterials: Synthesis, Characterization, and Application* (Elsevier Inc. 2016)
7. A.G. Korotkikh, O.G. Glotov, V.A. Arkhipov, V.E. Zarko, A.B. Kiskin, *Combust. Flame*, **178** (2017)
8. A. Abraham, H. Nie, M. Schoenitz, A.B. Vorozhtsov, M.I. Lerner, A. Pervikov, N. Rodkevich, E.L. Dreizin, *Combust. Flame*, **173** (2016)
9. V.A. Arkhipov, A.G. Korotkikh, V.T. Kuznetsov, A.A. Razdobreev, I.A. Evseenko, *Russ. J. Phys. Chem. B*, **5**, 4 (2011)
10. T.R. Sippel, S.F. Son, L.J. Groven, S. Zhang, E.L. Dreizin, *Combust. Flame*, **162** (2015)
11. V.A. Arkhipov, A.G. Korotkikh, *Combust. Flame*, **159** (2012)